

# Molecular Docking Analysis and Apoptotic Potential of Biosynthesized Silver Oxide Nanoparticles with Caspase-3

Ambika Behera<sup>1,\*</sup>, Shruti Awasthi<sup>2</sup>

<sup>1,2</sup>*Department of Life Science, Garden City University, Bangalore, (India)*

## ABSTRACT

This study analysed the molecular docking of the SilverOxide Nanoparticles (Ag<sub>2</sub>O-NPs) synthesized from the novelmedicinal plant Lagerstroemia indica.The formation of Ag<sub>2</sub>O-NPs was observed at a peak of 446 nm by the Ultraviolet-Visible (UV-Vis) spectrophotometerand the particle size was found to be9.98 nmby the X-Ray Diffraction (XRD) spectroscopy. Spherical-shaped NPs were detected from the Scanning Electron Microscope (SEM) images and the compound purity was observed from Energy Dispersive Spectroscopy (EDS) analysis. The weight percentage of Ag and O were found to be73.64 and 26.36, respectively. The atomic percentage of Ag and O were 29.29 and 70.71, respectively. The molecular docking of Caspase-3 was performed to determine the binding affinities of the Ag<sub>2</sub>O-NPs which helps in analysingthe apoptoticpotentialon human cancer cell lines.

**Keywords:** *Nanoparticles, Characterisation, Molecular docking, Silver oxide, Caspase-3*

## 1. Introduction

Cancer is one of the fearful disease, the principal cause of many deaths [1], always endup in compromised immune system [2-5]. The introduction of Nanotechnology hassignificantly enhanced the therapeutic efficacies [6-8] by bringing out the new self-assembled Nanoparticles (NPs) with negligible side effects which helps with an improved survival rate among cancer patients [9]. These nanomaterials (1-100 nm in sizes) are target-specific, can be encapsulated with other drugs and avert early degradation of drugs[10]. Amng other metal oxides, Silver oxide (Ag<sub>2</sub>O) has unique optical and thermal properties that are incorporated into products like, conducting ink, fillers and pastes for their high electrical conductivity and stability [11]. Ag<sub>2</sub>Oisalso used in the field of molecular diagnostics and photonic devices [12], in antibiotics [13], anticancer therapies [14], cosmetics [15], etc.So, in this study the crystallographic structure of Ag<sub>2</sub>O was selectedas a ligand from Protein Data Base (PDB) for the proposed docking study.

Molecular docking is a method which helps in the prediction of the appropriate confirmation, affinity and activity of a molecule to a targeted protein[16, 17]. It is a computational simulationbetween aligand and a proteinto achieve an energetic interaction [18, 19]. The modelobtained from this interaction is used to forecast the binding sites of protein[20, 21]. After the ligand and protein retrieved from the PDB [22, 23], the 3D structure of was drawn with the help of Chems sketch software and optimized by AutoDock open-source software [24]. In this study, the synthesized Ag<sub>2</sub>O-NPs has been used as the ligand and Caspase-3 (inhibitor isatin sulfonamide) was considered as the protein which was retried from PDB.

Apoptosis plays a key role in the normal growth and development of cells [25]. It is a programmed cell death which serves in the removal of unwanted cells and helps in smoothly carrying out the internal physiological functions. This mechanism functions by damaging the DNA, through cytokine deprivation [26] and by inducing death signals to cytotoxic T-cells from the immune system to all types of cells [27]. Once apoptosis is triggered, the activation of caspases will be activated which cleave irregular cell components for proper cellular functions [28]. Caspases are cysteine-aspartyl-specific proteases which are essential for apoptosis and encoded by CASP3 gene [29]. The catalytic sites include Cys-285, His-237, Gly-238 [30]. Caspases are used to prefer the peptide sequence of Asp-Glu-Val-Asp-Gly [31]. Caspase inhibitors are also known to target cell death. Isatin sulphonamides are potent and non-peptide Caspase-3 inhibitors [32].

In this study, the Ag<sub>2</sub>O-NPs has been synthesized from *L. indica* and the synthesized NPs has been characterized by various analytical methods. The 3D crystal structure of Caspase-3 complexed with isatin sulfonamide has been retrieved from PDB. It was docked with the synthesized Silver Oxide Nanoparticles (Ag<sub>2</sub>O-NPs) as ligand to study its anti-cancer potential.

## 2. Materials and Methods

### 2.1. Materials

In this work, the leaves of *L. indica* were selected and identified by the Herbarium of Botany Department, Garden City University (GCU), Bangalore. Silver Nitrate (AgNO<sub>3</sub>), Deionized Water (DW) and ethanol were procured from M/s Merck, India for the synthesis of Ag<sub>2</sub>O-NPs.

### 2.2. Preparation of Plant Extract

The collected healthy leaves were washed with DW and dried for a couple of weeks. The dried leaves were powdered and 3 g of the powdered extract mixed with 125 ml DW. After the solution was boiled at 70°C, it was cooled at room temperature and the solution was filtered. The filtrate was kept in a flask for further experimental needs.

### 2.3. Synthesis of Silver Oxide Nanoparticles

In a 250 ml flask, 90 ml of 1 mM AgNO<sub>3</sub> was added with 10 ml aqueous leaf extract. The solution was covered with aluminum foil to avoid photo-degradation and kept in a magnetic stirrer for 1 hour at 500 rpm. It was again kept under probe sonicator considering the following parameters, Pulse on: 50, Pulse off: 10 and Amplitude: 50% for 15 minutes, followed by magnetic stirrer at 400 rpm for 15 minutes. With the reaction, the color of the mixture changed from colorless to pale yellow to dark brown. The dark brown coloration confirmed the formation of Ag<sub>2</sub>O-NPs.

### 2.4. Characterization of Silver Oxide Nanoparticles

The obtained Ag<sub>2</sub>O-NPs were characterized in the absorption range of 350–500 nm in Ultraviolet-Visible (UV-Vis) spectrophotometer. The X-Ray Diffraction (XRD) Spectroscopy determined the particle size using CuK $\alpha$  radiation at ambient temperature and the shape of the particle was analyzed from Scanning Electron

Microscope (SEM). The elemental analysis of the compound  $\text{Ag}_2\text{O}$  was obtained from Energy Dispersive Spectroscopy (EDS).

### 2.5. Molecular Docking Analysis of SilverOxide Nanoparticles

Molecular docking is a computational tool to define an appropriate configuration between the drug and a protein. In this analysis, the crystal structure of Caspase-3 was retrieved from the PDB and its three-dimensional (3D) structure was constructed using the AutoDock module. Then, the active pocket site residues were constructed. Also, the 3D structure of the ligand was also prepared using Open Babel 2.4.1 and saved as pdb file format. Using CHARMM simulation module, the interaction energy score was achieved from the interaction of Ligand-Protein complex. In future, the highest interaction energy score can be taken into consideration which will be used in the prediction of physiological affinities of a molecule to a target protein for therapeutic approach towards anti-cancer agent.

## 3. Results and Discussion

### 3.1. Characterization of $\text{Ag}_2\text{O}$ -NPs

The formation of  $\text{Ag}_2\text{O}$ -NPs was confirmed at absorbance of 446 nm by the UV-Vis spectrophotometer (Fig.1). The diffraction peaks obtained from XRD analysis completely coordinated with the available JCPDS card No. 03-0921 (Fig. 2). These diffraction peaks ( $2\theta$ ) indicate that the synthesized  $\text{Ag}_2\text{O}$ -NPs have Face-Centered Cubic (FCC) structure of crystalline in nature.

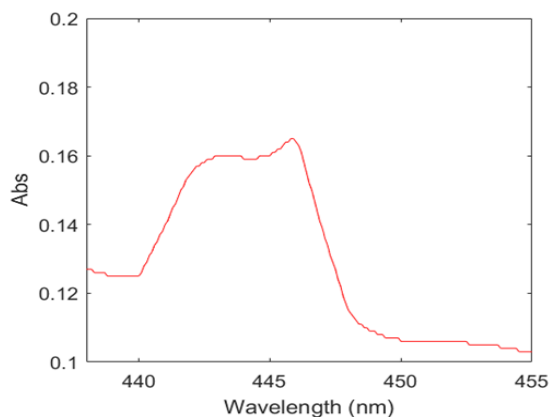


Fig.1. UV-Vis spectroscopy of  $\text{Ag}_2\text{O}$ -NPs.

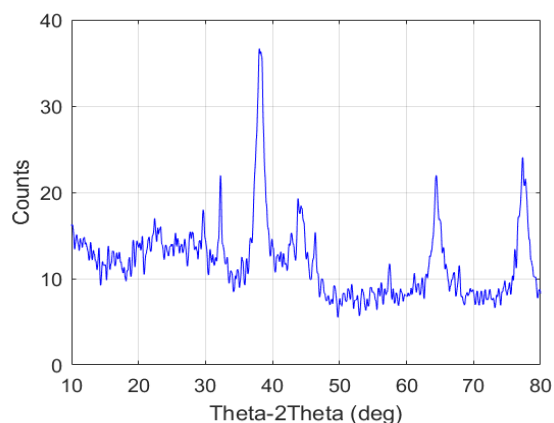


Fig.2. XRD analysis of  $\text{Ag}_2\text{O}$ -NP

From the graph, the  $2\theta$  values of  $32.21^\circ$ ,  $38.14^\circ$ ,  $46.35^\circ$ ,  $64.415^\circ$  and  $77.29^\circ$  can be indexed with (1 1 0), (1 1 1), (2 0 0), (2 2 0) and (3 1 1) planes. Using Debye-Scherrer's formula,

$$\text{Crystallite Size } (D) = \frac{0.89\lambda}{d \cos \theta} \quad (1)$$

the crystallite size ( $D$ ) calculated was 9.98 nm where, ( $\theta$ ) Bragg's diffraction angle, (0.89) Scherrer's constant, ( $\lambda = 0.154$ ) wavelength of X-rays, and ( $d$ ) Full Width at Half Maximum of  $2\theta$ . From Fig. 3(a) of SEM images, it was observed that most particles were aggregated in one place and found to be spherical in shape.

From the EDS micrograph in Fig.3 (b), the weight percentage of Ag and O were obtained as 73.64 and 26.36, respectively. The atomic percentage of Ag and O were 29.29 and 70.71, respectively.

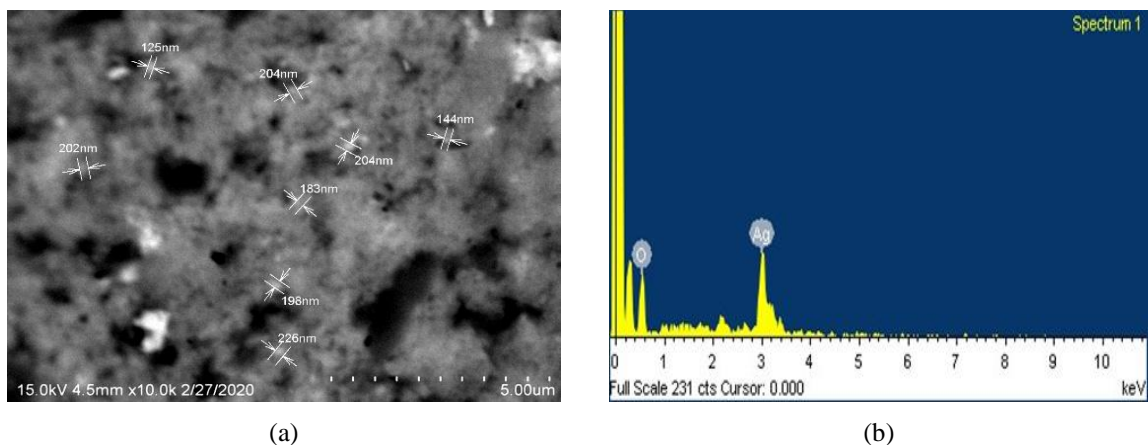


Fig.3. (a) SEM and (b) EDS images of Ag<sub>2</sub>O-NPs

### 3.2. Molecular Docking Analysis

#### 3.2.1. Protein Preparation

Using AutoDocktool, the crystal structure of Caspase-3 along with the inhibitor (isatin sulfonamide) was retrieved from PDB at 2.8 Å resolution (Fig.4).Molecular weight of the protein was found to be 27,375.2 from the received data. The total number of amino acid residues was found to be 238 and the amino acid chain named as AB. In the next step, water molecules were removed using clean protein protocol, polar and non-polar hydrogen atoms were added, Gasteiger charges were figured and finally, the file was saved as pdbqt file (Fig.5). From the protein preparation, -14311.70998 kcal/mol of the potential energy, -1762.12583 kcal/mol of Vander Waals energy and Root Mean Square (RMS) energy of 0.96320 kcal/mol were obtained. With Smart Minimizer algorithm, the energy is minimized to 1000 steps and RMS gradient energy is reduced to 0.1.



Fig.4. Caspase-3 complex with isatin sulfonamide inhibitor

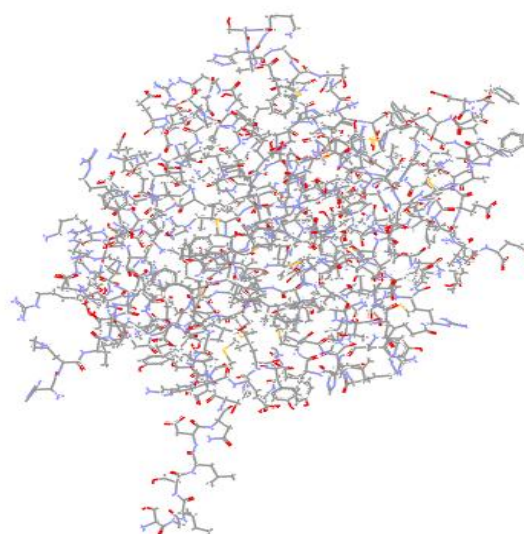


Fig. 5. Prepared Protein structure

### 3.2.2. Preparation of Ligand

Using ACD/ChemSketch of 12.0, the 2D structure of  $Ag_2O$  was drawn in mol.file format and with the help of Open Babel 2.4.1, it was converted to a 3D structure and saved as pdb file format. The water molecules were removed, hydrogen atoms were added, torsion was defined and the Gasteiger charges were added (Fig. 6).

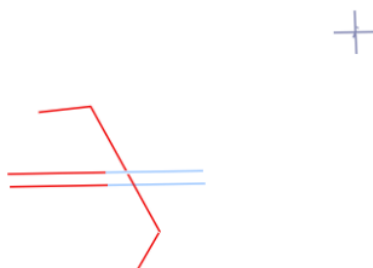


Fig.6. Prepared structure of Ligands

### 3.2.3. Binding Sites on Protein

In Fig.7, the binding sites of the protein were identified by Define and Edit Binding Site tool. The best active binding sites were identified and docked with the ligand  $Ag_2O$ . The binding sites identified were: MET61 ARG207 LYS57 SER205 SER58 PHE256 TRP206 GLY122 TYR204 HIS121 CYS163

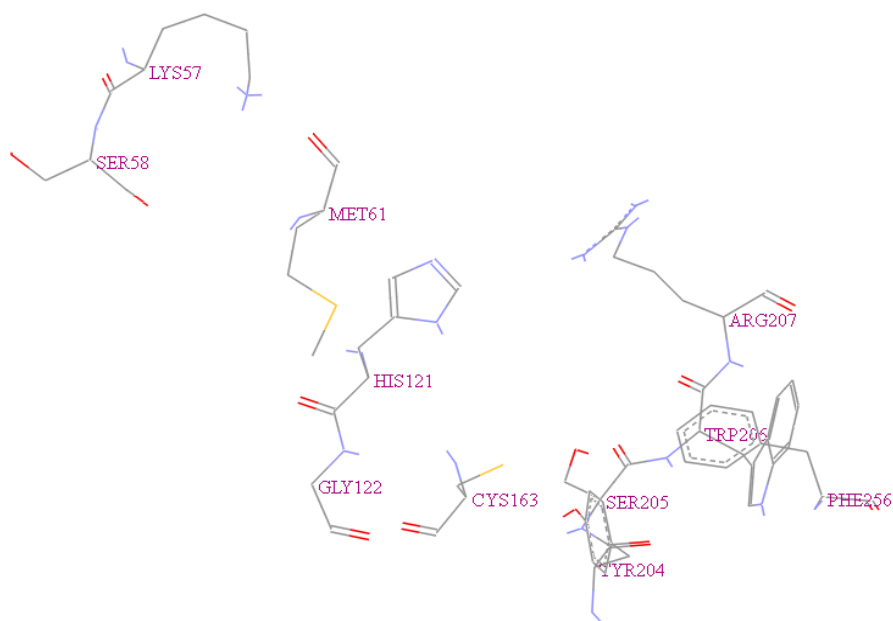


Fig.7. Binding sites of 1gfw

### 3.2.4. Molecular Docking Result

Using AutoDock 4.2.6, the docking of ligand was performed into the protein (Caspase-3) binding sites (as shown in Fig.8) to determine the affinities of the complex formed. The complex achieved a high interaction energy of 0.9 kcal/mol and a binding energy of -0.96931 kcal/mol.

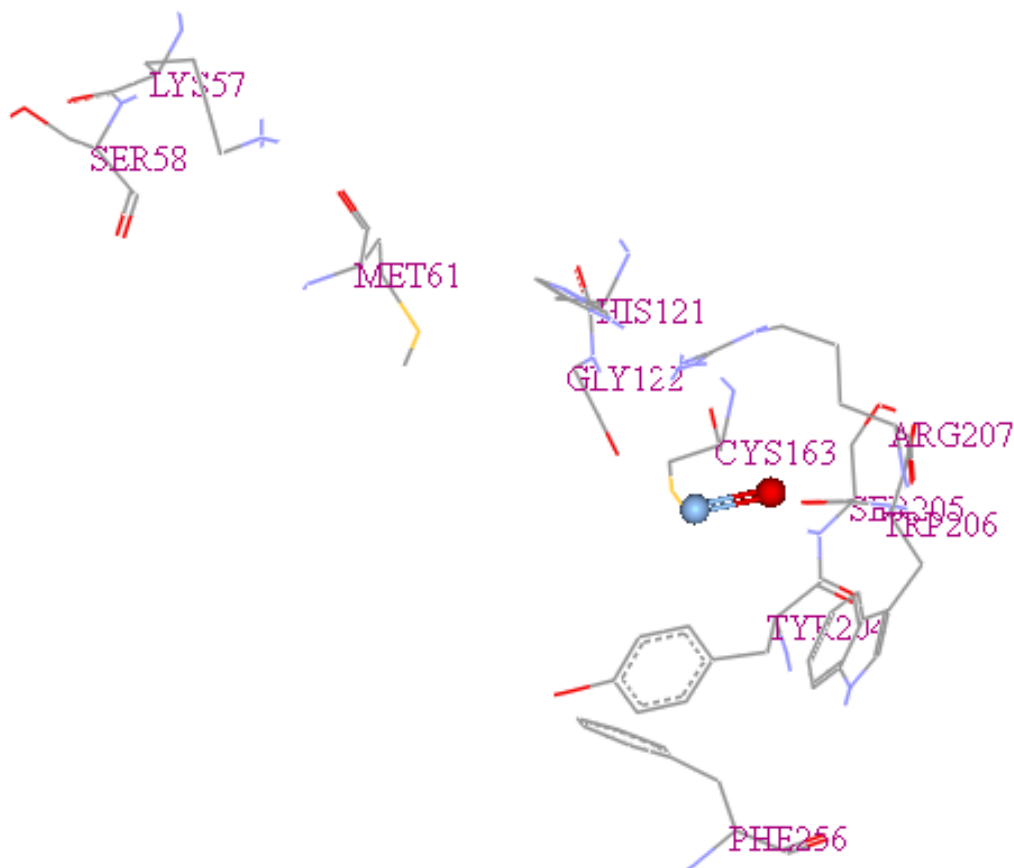


Fig.8. Protein-Ligand interaction

#### 4. Conclusion

This study analysed the molecular docking of the apoptotic Caspase-3 with the synthesized silver oxide nanoparticles ( $\text{Ag}_2\text{O}$ -NPs) from the novel plant, *Lagerstroemia indica*. The formation of  $\text{Ag}_2\text{O}$ -NPs at a peak of 446 nm was observed by UV-Vis spectroscopy. The SEM images confirmed the spherical-shaped NPs and the purity of  $\text{Ag}_2\text{O}$  compound was determined by EDS micrographs. The crystallinity of NPs was found to be Face-Centered Cubic (FCC) structure by XRD analysis and the average crystallite size was calculated as 9.98 nm. The docking analysis of  $\text{Ag}_2\text{O}$  with Caspase-3 has been achieved with -0.96931 kcal/mol binding energy. Thus, the present study suggests the use of  $\text{Ag}_2\text{O}$ -NPs as a potent drug against various cancer diseases by targeting the apoptotic pathway.

#### 5. Acknowledgement

The authors thank The Chancellor, Garden City University, Bangalore for institutional support and Averin Biotech Biotechnology Training Company, Hyderabad for analytical tests and cytotoxicity experiments.

#### References

- [1] R.L. Siegel and K.D. Miller, A. Jemal, Cancer statistics, *CA Cancer J. Clin.*, 70(1), 2020, 7–30.
- [2] R. Bazak, M. Hourri, S. El Achy, *et al.*, Passive targeting of nanoparticles to cancer: A comprehensive review of the literature, *Mol Clin Oncol*, 2(6), 2014, 904-908.

- [3] J.D. Byrne, T. Betancourt and L. Brannon-Peppas, Active targeting schemes for nanoparticle systems in cancer therapeutics, *Adv Drug Deliv Rev*, 60(15), 2008, 1615-1626.
- [4] P.N. Navya, A. Kaphle and H.K. Daima, Nanomedicine in sensing, delivery, imaging and tissue engineering: advances, opportunities and challenges. *Nanosci*, 5, 2019, 30–56.
- [5] R.A. Revia and M. Zhang, Magnetite nanoparticles for cancer diagnosis, treatment, and treatment monitoring: recent advances. *Mater. Today*, 19(3), 2016, 157–168.
- [6] X. Han, K. Xu, O. Taratula, *et al.*, Applications of nanoparticles in biomedical imaging, *Nanoscale*, 11, 2019, 799-819.
- [7] M.J.D. Esmatabadi, B. Bakhshinejad, F.M. Motlagh, *et al.*, Therapeutic resistance and cancer recurrence mechanisms: Unfolding the story of tumour coming back, *J Biosci*, 41(3), 2016, 497-506.
- [8] O. Jain, Applications of nanoparticles in biology and medicine, *J Nanobiotechnology*, 2(3), 2004.
- [9] P.K. Jain, K.S. Lee, I.H. El-Sayed, *et al.*, Calculated absorption and scattering properties of gold nanoparticles of different size, shape, and composition: applications in biological imaging and biomedicine, *J Phys Chem B*, 110(14), 2006, 7238-7248.
- [10] R. Ostermann, J. Cravillon, C. Weidmann, *et al.*, Metal–organic framework nanofibers via electrospinning, *Chem. Commun*, 47(1), 2011, 442–444.
- [11] W. Wei, X. Mao, L. A. Ortiz, *et al.*, Oriented silver oxide nanostructures synthesized through a template-free electrochemical route, *J Mater Chem*, 21(2), 2011, 432–438.
- [12] N. L. Yong, A. Ahmad, and A. W. Mohammad, Synthesis and characterization of silver oxide nanoparticles by a novel method, *Int J Sci Eng Res*, 4(5), 2013, 155–158.
- [13] V. Manikandan, Green synthesis of silver oxide nanoparticles and its antibacterial activity against dental pathogens, *3 Biotech*, 7(72), 2017.
- [14] A. A. Rokade, M. P. Patil, S. I. Yoo, *et al.*, Pure green chemical approach for synthesis of Ag<sub>2</sub>O nanoparticles, *Green Chem Lett Rev*, 9(4), 2016, 216–222.
- [15] M. Yadav, R.S. Lawrence RS, M. Jalees, *et al.*, Biological synthesis and antibacterial activity of silver oxide nanoparticle prepared from Carica papaya root extract, *Int J Pure App Biosci*, 6(2), 2018, 1632–1639.
- [16] B.G. Vijayakumar, D. Ramesh, A. Joji, *et al.*, In silico pharmacokinetic and molecular docking studies of natural flavonoids and synthetic indole chalcones against essential proteins of SARS-CoV-2, *Eur J Pharmacol*, 886(5), 2020, 173448.
- [17] Niveshika, S. Singh, E. Verma, *et al.*, In silico molecular docking analysis of cancer biomarkers with GC/MS identified compounds of *Scytonema* sp., *Netw Model Anal Health Inform Bioinforma*, 9(30), 2020.
- [18] H. Tsujikawa, K. Sato, C. Wei, *et al.*, Development of a protein–ligand-binding site prediction method based on interaction energy and sequence conservation. *J Struct Funct Genomics*, 17(2), 2016, 39–49.
- [19] P. Pandey, R. Srivastava and P. Bandyopadhyay, Comparison of molecular mechanics-Poisson-Boltzmann surface area (MM-PBSA) and molecular mechanics-three-dimensional reference interaction site model (MM-3D-RISM) method to calculate the binding free energy of protein-ligand complexes: Effect of metal ion and advance statistical test, *Chem Phys Lett*, 695, 2018, 69-78.

- [20] M. Brylinski and W.P. Feinstein, eFindSite: Improved prediction of ligand binding sites in protein models using meta-threading, machine learning and auxiliary ligands, *J Comput Aided Mol Des*, 27(6), 2013, 551–567.
- [21] J. Zhao, Y. Cao and L. Zhang, Exploring the computational methods for protein-ligand binding site prediction, *Comput Struct Biotechnol J*, 18, 2020, 417-426.
- [22] J.D. Tyzack, L. Fernando, A.J.M. Ribeiro, *et al.*, Ranking enzyme structures in the PDB by bound ligand similarity to biological substrates, *Structure*, 26(4), 2018, 565-571.
- [23] Y. Murakami, S. Omori and K. Kinoshita, NLDB: a database for 3D protein-ligand interactions in enzymatic reactions, *J Struct Funct Genomics*, 17(4), 2016, 101-110.
- [24] E.L. Gelamo, C.H.T.P. Silva and H. Imasato, *et al.*, Interaction of bovine (BSA) and human (HSA) serum albumins with ionic surfactants: spectroscopy and modelling, *Biochim. Biophys. Acta*, 1594(1), 2002, 84–99.
- [25] A.B. Parrish, C.D. Freel and S. Kornbluth, Cellular mechanisms controlling caspase activation and function, *Cold. Spring. Harb. Perspect. Biol*, 5(6), 2013, a008672.
- [26] S. Zaman, R. Wang and V. Gandhi, Targeting the apoptosis pathway in hematologic malignancies, *Leuk Lymphoma*. 55(9), 2014, 1980-1992.
- [27] M. Hassan, H. Watari, A. AbuAlmaaty, *et al.*, Apoptosis and molecular targeting therapy in cancer, *Biomed Res Int*, 2014, 150845.
- [28] J. Lopez and S.W. Tait, Mitochondrial apoptosis: killing cancer using the enemy within, *Br J Cancer*, 112(6), 2015, 957-962.
- [29] V. Ranwez, F. Delsuc, S. Ranwez, *et al.*, OrthoMaM: A database of orthologous genomic markers for placental mammal phylogenetics, *BMC Evol Biol*, 7 (241), 2007, 1-12.
- [30] I.N. Lavrik, A. Golks, and P.H. Krammer, Caspases: Pharmacological manipulation of cell death, *J. Clin. Invest*, 115(10), 2005, 2665–2672.
- [31] S.R. D'Mello, C.Y. Kuan, R.A. Flavell, *et al.*, Caspase-3 is required for apoptosis-associated DNA fragmentation but not for cell death in neurons deprived of potassium, *J Neurosci Res*, 59(1), 2000, 24-31.
- [32] M.S. Ayoup, Y. Wahby, H. Abdel-Hamid, *et al.*, Design, synthesis and biological evaluation of novel  $\alpha$ -acyloxy carboxamides via Passerini reaction as caspase 3/7 activators, *Eur J Med Chem*, 168, 2019, 340–356.